On Channel Equalization for Full-duplex Relay Networks

Konstantin Muranov
University of Illinois at Chicago
kmuran2@uic.edu

Besma Smida
Senior Member, IEEE
University of Illinois at Chicago
smida@uic.edu

Natasha Devroye
Senior Member, IEEE
University of Illinois at Chicago
devroye@uic.edu

***Abstract*—In this paper we analyze the performance of a full-duplex relay system in the presence of residual self-interference (SI) and frequency-selective fading. In particular, the residual SI channel estimation performance is evaluated both analytically and via simulation. The bit error rate (BER) performance at the destination is also characterized via simulation. Two schemes are considered for the equalization of the source-to-relay (SR) and relay-to-destination (RD) channels: end-point equalization and distributed equalization. In the first approach, channel equalization is performed only at the destination and is similar to an amplify-and-forward model. In the second approach, equalization of the SR channel is performed at the relay, while the RD channel equalization is performed at the destination. We show that at the cost of a modest complexity increase at the relay, the distributed scheme provides more robust performance than its end-point counterpart.**

I. Introduction

Wireless relay systems can improve network coverage and data rates at the expense of moderate increase in system complexity. This is becoming more relevant in light of the recent interest in utilizing the Extremely High Frequency (EHF) band, which is highly susceptible to atmospheric attenuation. As a result, research community has been devoting more attention to devising spectrally-efficient communication schemes using two-way relays, while the communication industry standards have also been incorporating relays into their systems. The transmitter and receiver of a single half-duplex (HD) node employ orthogonal channels to avoid interfering with one another. This orthogonality is achieved by utilizing different frequencies, time slots, or orthogonal spread-spectrum codes. In contrast, the transmitter and receiver of a full-duplex (FD) system operate on the same channel, which can significantly improve spectral efficiency at the expense of increased transceiver complexity.

Due to the recent advances in the area of FD transceivers [1], [3], [5], [15] and due to their ability to achieve higher spectral efficiency, full-duplex transceivers are increasingly being considered for use in a variety of scenarios. For example, [2] and [12] considered applicability of FD base stations in cellular networks. Full-duplex wireless relaying is another context where full-duplex transceivers find natural application. A two-hop full-duplex relaying system could consist of a source node, FD relay node, and destination. That is, the source-relay and relay-destination radio links use the same frequency channel at the same time. Such FD relay nodes could be seamlessly inserted between the source and destination nodes with minimum impact on the system configuration. However, introduction of the relay node into the system, increases the propagation delay (due to the processing delay at the relay) and changes characteristics of the end-to-end propagation channel seen by the destination receiver.

The feasibility of using full-duplex relaying was initially studied in [9] and [7], where the end-to-end capacity expressions were derived for amplify-and-forward (AF) and decode-and-forward (DF) full-duplex relay systems. It was shown that FD relay schemes provided end-to-end channel capacity improvement relative to their HD counterparts when residual SI levels were below certain *break-even* levels. Furthermore, it was found that the break-even levels vary depending on the normalized gains of the source-relay (SR) and relay-destination (RD) channels as well as the power levels at the source and relay transmitters. Expressions outlining this dependence were derived. Since then, a number of SI mitigation techniques were offered, specifically in the context of full-duplex relaying. The spatial SI suppression in MIMO-based full-duplex AF relay and the impact of the SI channel estimation errors were considered in [6], where it was shown that methods that suppress SI while maximizing SIR at the relay transmitter and receiver provide better channel capacity performance than zero-forcing methods focusing only on SI suppression. The combination of time-domain cancellation and spatial suppression techniques such as null-space projection, antenna and beam selection were evaluated in [8]. It was concluded that these techniques provide sufficient SI mitigation and that FD relay systems can ensure reliable communication link.

Contributions. In this paper we focus on the effect of equalization in a full-duplex relaying system in the presence of residual self-interference. Specifically, we derive the Cramer-Rao Lower Bound (CRLB) for the SI channel estimator and use it in order to analyze the effect that presence or absence of channel equalization at the relay would have on the end-to-end performance of full-duplex relay system. To that end, we compare performance of two system configurations: 1)

The work of B. Smida was partially supported by NSF CAREER award 1620902

The work of N. Devroye was partially supported by NSF under award 1053933

978-1-4673-8999-0/17/$31.00 ©2017 IEEE

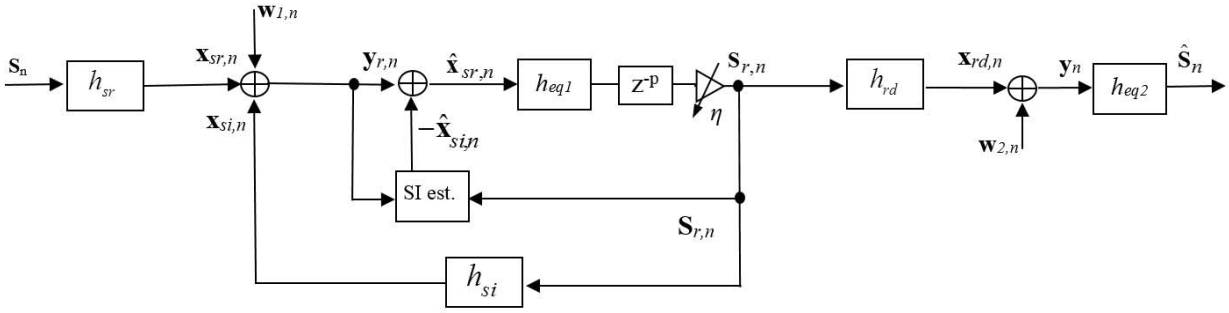

Fig. 1. Simplified full-duplex relay system

distributed channel equalization, where in addition to SI mitigation, the SR channel equalization is performed at the relay, while RD channel equalization is performed at the destination; 2) *end-point channel equalization*, where only SI mitigation and signal amplification are performed at the relay and channel equalization is performed only at the destination node. Our findings indicate that as long as no significant amount of noise is introduced at the relay transmitter and assuming sufficient dynamic range of the digital signal representation, an efficient SI channel estimator can be constructed, resulting in end-to-end BER performance comparable to half-duplex case. Also, according to simulation results, the presence of SR channel equalization at the relay results in performance that is superior to the end-point configuration. It is our understanding that this problem has not been investigated in the literature. This work has another unique feature: the digital processing at the relay does not include hard-decision as part of the symbol detection. However, unlike [13], log likelihood ratio values are not estimated at the relay. Instead, the relay performs digital-to-analog conversion of the processed signal samples. This avoids decoding and re-encoding of the data at the relay, which can be costly in terms of complexity and processing delay. Absence of the channel equalization at the relay in the case of end-point configuration, would result in a wide range of transmitted sample amplitude. In a practical system, this would certainly cause dynamic range issues at both relay transmitter and destination receiver. However, for the purpose of this investigation, we assumed unlimited dynamic range. Finally, the end-to-end BER performance of the end-point and distributed configurations is evaluated at different SI levels via link simulation.

II. System Model and Notation

Notation. In the remainder of the text, vectors and matrices are represented by bold lower-case and upper-case letters, respectively. In the case of signal vectors, the index provided in the subscript represents the index of the first element within the vector. For example, the vector form of the additive noise sequences at the relay and destination receivers are denoted as $\mathbf{w}_{1,n} = \big[w_1[n], \ldots, w_1[n+A-1]\big]^T$ and $\mathbf{w}_{2,n} = \big[w_2[n], \ldots, w_2[n+A-1]\big]^T$, where A represents the symbol block size used for computing a single estimate. Both noise signals are assumed to be complex Gaussian, white, and stationary: $\mathbf{w}_{1,n} \sim \mathcal{N}(\mathbf{0}, \sigma_1^2\mathbf{I})$ and $\mathbf{w}_{2,n} \sim \mathcal{N}(\mathbf{0}, \sigma_2^2\mathbf{I})$. In the case of channel vectors, the index in the subscript has a different meaning representing the channel realization at the sampling instance n.

Channel model. The convolution operation will be represented as a product of a filtering matrix and a vector. Hence, output of the SI channel can be given by $\mathbf{S}_{r,n}\mathbf{h}_{si,n}$, where $\mathbf{S}_{r,n}$ is the filtering matrix composed of the samples transmitted by the relay and can be represented in the following column form:

$$\mathbf{S}_{r,n} = \big[\mathbf{s}_{r,n}^{(0)}, \mathbf{s}_{r,n}^{(1)}, ..., \mathbf{s}_{r,n}^{(M)}\big], \tag{1}$$

where M is the order of the SI channel impulse response, and individual columns are defined as,

$$\mathbf{s}_{r,n}^{(0)} = \begin{bmatrix} s_r[n] \\ s_r[n+1] \\ \vdots \\ s_r[n+A-1] \end{bmatrix}, \quad \mathbf{s}_{r,n}^{(1)} = \begin{bmatrix} 0 \\ s_r[n] \\ \vdots \\ s_r[n+A-2] \end{bmatrix}, \quad ...$$

The channel vector is defined as $\mathbf{h}_{si,n} = \big[h_{si,n}[0], \ldots, h_{si,n}[M]\big]^T$, where $A >> M$. Alternatively, the same convolution operation can also be represented by a product of channel filtering matrix and vector of signal samples: $\mathbf{H}_n\mathbf{s}_n$, with dimensions $\mathbf{s}_n : (A+M) \times 1$ and $\mathbf{H}_n : A \times (A+M)$, and

$$\mathbf{H}_n = \begin{bmatrix} h_n[M] & h_n[M-1] & ... & h_n[0] & 0 & 0 \ ... & 0 \\ 0 & h_n[M] & ... & h_n[1] & h_n[0] & 0 \ ... & 0 \\ \vdots & \vdots & & \vdots & & & \vdots \\ 0 & 0 & ... & 0 & 0 & 0 \ ... & h_n[0] \end{bmatrix}.$$

FD relay system is depicted in Fig. 1, where it is assumed that there is no direct link from source to the destination, and where the signal received at the relay is defined as,

$$\begin{aligned} \mathbf{y}_{r,n} &= \mathbf{S}_n\mathbf{h}_{sr,n} + \mathbf{S}_{r,n}\mathbf{h}_{si,n} + \mathbf{w}_{1,n}, \\ &= \mathbf{x}_{sr,n} + \mathbf{x}_{si,n} + \mathbf{w}_{1,n}. \end{aligned} \tag{2}$$

The signal received at the destination is given by,

$$\mathbf{y}_n = \mathbf{S}_{r,n}\mathbf{h}_{rd,n} + \mathbf{w}_{2,n}. \tag{3}$$

In the above expression, $\mathbf{h}_{sr,n}, \mathbf{h}_{si,n}$, and $\mathbf{h}_{rd,n}$ represent impulse responses of the source-to-relay, self-interference, and relay-to-destination wireless propagation channels, respectively. We call them composite since they incorporate propagation, receiver, and transmitter components. All channels are assumed to be stationary with a finite impulse response. For simplicity, the order of all channel impulse response (CIR) functions is assumed to be identical and equal to M. The vectors representing their respective output signals are given by, $\mathbf{x}_{sr,n}, \mathbf{x}_{si,n}$, and $\mathbf{x}_{rd,n}$, where n is the sampling instance corresponding to the first element of the vector.

$\mathbf{S}_n$ and $\mathbf{S}_{r,n}$ represent filtering matrices composed of symbols transmitted by the source and samples transmitted by the relay. It is assumed that QPSK-modulated symbols are transmitted by the source. $\mathbf{h}_{eq1,n}, \mathbf{h}_{eq2,n}$ represent the impulse responses of the fractionally-spaced MMSE equalizers at the relay and destination respectively. Defining the SI channel in terms of the gain factor, γ_{si}, and normalized channel, $\tilde{\mathbf{h}}_{si}$, as $\mathbf{h}_{si} = \gamma_{si}\tilde{\mathbf{h}}_{si}$ and assuming that channel impulse responses $\tilde{\mathbf{h}}_{si}$, $\mathbf{h}_{sr,n}$, and $\mathbf{h}_{rd,n}$ are normalized to unity gain, the SINR at the relay receiver may be defined as follows

$$SINR_r = \frac{\mathbb{E}(\|\mathbf{x}_{sr}\|^2)}{\mathbb{E}(\|\mathbf{x}_{si}\|^2) + \mathbb{E}(\|\mathbf{w}_1\|^2)} = \frac{1}{\gamma_{si}^2 + \sigma_{w1}^2}. \quad (4)$$

The signal-to-self-interference ratio is defined as, $\frac{P_{sr}}{P_{si}} = \frac{1}{\gamma_{si}^2}$, where P_{sr} and P_{si} are the energies of the signals at the output of SR and SI channels, respectively. Then, the noise variance, σ_{w1}^2, can be expressed as

$$\sigma_{w1} = \sqrt{\frac{1}{SINR1} - \frac{1}{P_{sr}/P_{si}}} = \sqrt{\frac{1}{SINR1} - \gamma_{si}^2}. \quad (5)$$

Finally, η is the amplification factor at the relay transmitter. The processing delay within the relay is given by $p \in \mathbb{Z}$, measured in the multiples of the symbol interval.

In order to preserve as much information as possible about the symbols transmitted by the source node, once the channel equalization is performed at the relay, the symbols are not mapped back to the specific constellation points. However, in contrast to the methods described in [13], the log likelihood ratio values are not computed in our case. As shown in Fig. 1, the processed samples are passed directly to the relay transmitter, where signal is amplified achieving power level of γ_r^2. This is accomplished by scaling the estimated symbols $\hat{s}_r[n]$ by the factor η:

$$s_r[n] = \eta\hat{s}_r[n], \quad \text{where} \quad \eta = \gamma_r\sqrt{\frac{1}{\mathbb{E}\left(|\hat{s}_r[n]|^2\right)}}. \quad (6)$$

Two forms of equalization. We consider two configurations that can be defined as *end-point* and *distributed* equalization. The first scheme assumes that channel equalization is performed at the destination only, and the digital processing at the relay only involves residual SI estimation and cancellation. In contrast, under the distributed equalization approach, the channel equalization is performed both at the relay and destination. In this case, the residual SI cancellation is followed by channel equalization. It is possible to estimate the SI and SR channels jointly at the relay. However, in order to facilitate comparison between end-point and distributed configurations, in this work we assume that in the distributed case, SI estimation and cancellation is performed first, followed by SR channel equalization.

Fig. 1 depicts the model for distributed equalization. The end-point model can be obtained by removing the block corresponding to $\mathbf{h}_{eq1}$ from the diagram.

Our main goal is to analyze the impact of the presence of the channel equalization at the relay on the SI estimation and end-to-end BER performance without regard to the method used for estimating other channels within the system. Hence, it is assumed that a perfect estimate of the SR and RD channels are available to the equalizers within the system.

SI estimation model. It is assumed that self-interference is reduced to a manageable level by antenna separation and analog cancellation techniques. The residual SI is then estimated and canceled digitally. The estimation of the SI channel at the relay is impaired not only by AWGN, but also by interference from the SR signal, $\mathbf{x}_{sr,n} = \mathbf{S}_n\mathbf{h}_{sr,n}$.

We assume that SI channel is linear and, in contrast to [10], [11], [15] there is no noise introduced at the the relay transmitter, resulting in perfect knowledge of the $\mathbf{s}_{r,n}$ by the relay. These assumptions are not totally accurate, but allow simplified analysis. Inclusion of the non-linear effects and noise into the model could be part of the future work.

The system equation (2) is valid for both end-point and distributed configurations. The difference between the two configurations is manifested in the definition of the signal, $\mathbf{s}_{r,n}$ and is due to the presence of SR channel equalization in distributed case. *End-point equalization:*

$$\mathbf{s}_{r,n} = \mathbf{H}_{sr,n-p}\mathbf{s}_{n-p} + \mathbf{w}_{1,n-p} + \mathbf{H}_{e,n}\mathbf{s}_{r,n-p} \quad (7)$$

Distributed equalization:

$$\begin{aligned}\mathbf{s}_{r,n} = {} & \mathbf{H}_{eq1,n-p}\mathbf{H}_{sr,n-p}\mathbf{s}_{n-p} + \mathbf{H}_{eq1,n-p}\mathbf{w}_{1,n-p} \\ & + \mathbf{H}_{eq1,n-p}\mathbf{H}_{e,n}\mathbf{s}_{r,n-p}, \end{aligned} \quad (8)$$

where $\mathbf{H}_{e,n} = \mathbf{H}_{si,n} - \hat{\mathbf{H}}_{si,n}$ represents SI channel estimation error. We can consider $\mathbf{x}_{sr,n}$, $\mathbf{w}_{1,n}$ in equation (2) as impairments to estimation of the SI signal. If we assume that the magnitude of $\mathbf{x}_{sr,n}$ samples follows Rayleigh PDF, this would imply that these samples have complex Gaussian PDF with zero mean. Hence, $\mathbf{w}_{eff,n} = \mathbf{x}_{sr,n} + \mathbf{w}_{1,n}$ is a sum of two independent Gaussian-distributed random vectors with different means and autocorrelation matrices (in both, end-point and distributed configurations):

$$\mathbf{x}_{sr,n} = \mathbf{H}_{sr,n}\mathbf{s}_n \sim \mathcal{N}(\mathbf{0}, \mathbf{C}_{sr}), \quad \mathbf{w}_{1,n} \sim \mathcal{N}(\mathbf{0}, \mathbf{I}\sigma_{w1}^2). \quad (9)$$

Hence, the effective noise vector, $\mathbf{w}_{eff}$, is also Gaussian [14]:

$$\mathbf{w}_{eff,n} = (\mathbf{H}_{sr,n}\mathbf{s}_n + \mathbf{w}_{1,n}) \quad \sim \mathcal{N}(\mathbf{0}, \mathbf{C}_{w_{eff}}). \quad (10)$$

Considering equation (2) in light of the above assumptions, we have $\mathbf{y}_{r,n} \sim \mathcal{N}(\mu_{y_r}, \mathbf{C}_{y_r})$, where

$$\mu_{y_r} = \mathbf{S}_{r,n}\mathbf{h}_{si,n} = \mathbf{S}_{r,n}\gamma_{si}\tilde{\mathbf{h}}_{si,n}, \quad (11)$$

and covariance matrices are

$$\begin{aligned}\mathbf{C}_{y_r} &= \mathbb{E}\left[(\mathbf{y}_r-\mu_{y_r})(\mathbf{y}_r-\mu_{y_r})^H\right]\\ &= \mathbb{E}\left[(\mathbf{H}_{sr,n}\mathbf{s}_n+\mathbf{w}_{1,n})(\mathbf{s}_n^H\mathbf{H}_{sr,n}^H+\mathbf{w}_{1,n}^H)\right]\\ &= \varepsilon_s\mathbf{H}_{sr,n}\mathbf{H}_{sr,n}^H+\mathbf{I}\sigma_{w1}^2. \end{aligned} \quad (12)$$

The residual SI channel estimation is assumed to be based on Linear Least Squares Estimator (LLSE):

$$\hat{\mathbf{h}}_{si,n}=\left(\mathbf{S}_{r,n}^H\mathbf{C}_{y_r}^{-1}\mathbf{S}_{r,n}\right)^{-1}\mathbf{S}_{r,n}^H\mathbf{C}_{y_r}^{-1}\mathbf{y}_{r,n}, \quad (13)$$

where $\mathbf{y}_{r,n}$ is the signal received at the relay (2), $\mathbf{S}_{r,n}$ is the filtering matrix composed by the samples transmitted by the relay and is defined in equation (1). The inclusion of covariance matrix $\mathbf{C}_{y_r}$ is due to the fact that estimation is performed in the presence of non-white complex Gaussian noise, $\mathbf{w}_{eff,n}$, consisting of the output of the SR channel and relay receiver noise. Under these conditions, the estimator given by expression (13) is considered to be efficient [4].

The estimated SI channel and the samples transmitted by the relay are used for generating an estimate of the SI signal as follows,

$$\hat{\mathbf{x}}_{si,n}=\mathbf{S}_{r,n}\hat{\mathbf{h}}_{si,n}, \quad (14)$$

which is then subtracted from the total received signal as shown in Fig. 1.

III. System Performance Analysis

A. SI Channel Estimation Performance

In this subsection we will derive the CRLB for SI channel estimation for both end-point and distributed configurations. The CRLB analysis at high SNR will indicate that presence of SR channel equalization at the relay improves the SI channel estimation performance. Specifically, we will show that in the noiseless case, the CRLB for *end-point model* is given by

$$[\mathrm{CRLB}(\mathbf{h}_{si})]_{ii}\,(\sigma_{w1}^2=0)\approx \varepsilon_s\left\{\mathbf{s}_{n-p}^H\mathbf{H}_{sr,n-p}^H\left[\mathbf{H}_{sr,n}\mathbf{H}_{sr,n}^H\right]^{-1}\mathbf{H}_{sr,n-p}\mathbf{s}_{n-p}\right\}^{-1},$$

while for *distributed model* it becomes,

$$[\mathrm{CRLB}(\mathbf{h}_{si})]_{ii}(\sigma_{w1}^2=0)\approx\varepsilon_s\left\{\mathbf{s}_{n-p}^H\left[\mathbf{H}_{sr,n}\mathbf{H}_{sr,n}^H\right]^{-1}\mathbf{s}_{n-p}\right\}^{-1}.$$

The SI channel estimation errors start having significant detrimental impact on the overall system performance only at high SNR since at lower and medium SNR levels, the performance is mainly limited by the noise. Hence, we focus on the noiseless case, where the SI estimation performance is the most critical.

Derivation: The PDF of the signal samples received at the relay has the following *complex Gaussian* form for both configurations:

$$f(\mathbf{y}_r;\mathbf{h}_{si})=\frac{1}{\pi^N det\left[\mathbf{C}_{y_r}\right]}\exp\Big\{-(\mathbf{y}_{r,n}-\mathbf{S}_{r,n}\mathbf{h}_{si,n})^H \times\mathbf{C}_{y_r}^{-1}(\mathbf{y}_{r,n}-\mathbf{S}_{r,n}\mathbf{h}_{si,n})\Big\}. \quad (15)$$

According to [4], Fisher information matrix (FIM) is given by,

$$\mathbf{J}(\mathbf{h}_{si})=-\mathbb{E}\left(\left[\frac{\partial\ln f(\mathbf{y}_r;\mathbf{h}_{si})}{\partial\mathbf{h}_{si}^*}\right]\left[\frac{\partial\ln f(\mathbf{y}_r;\mathbf{h}_{si})}{\partial\mathbf{h}_{si}^*}\right]^H\right). \quad (16)$$

$$\begin{aligned}[\mathbf{J}(\mathbf{h}_{si})]_{i,j}=&\,tr\left[\mathbf{C}_{y_r}^{-1}\frac{\partial\mathbf{C}_{y_r}}{\partial\mathbf{h}_{si}^*[i]}\mathbf{C}_{y_r}^{-1}\frac{\partial\mathbf{C}_{y_r}}{\partial\mathbf{h}_{si}[j]}\right]\\ &+\left(\frac{\partial\mathbf{S}_{r,n}\mathbf{h}_{si,n}}{\partial\mathbf{h}_{si,n}^*[i]}\right)^H\mathbf{C}_{y_r}^{-1}\left(\frac{\partial\mathbf{S}_{r,n}\mathbf{h}_{si,n}}{\partial\mathbf{h}_{si,n}^*[j]}\right)\\ &+\left(\frac{\partial\mathbf{S}_{r,n}\mathbf{h}_{si,n}}{\partial\mathbf{h}_{si,n}[i]}\right)^H\mathbf{C}_{y_r}^{-1}\left(\frac{\partial\mathbf{S}_{r,n}\mathbf{h}_{si,n}}{\partial\mathbf{h}_{si,n}[j]}\right). \end{aligned} \quad (17)$$

Since $\mathbf{C}_{y_r}$ is independent of $\mathbf{h}_{si,n}$ and $\partial h_{si,n}[i]/\partial h_{si,n}^*[i]=0$, the first two terms in expression (17) become zeros, we have

$$\begin{aligned}\mathbf{J}(\mathbf{h}_{si})=&\,\mathbf{S}_{r,n}^H\mathbf{C}_{y_r}^{-1}\mathbf{S}_{r,n}\\ =&\,\mathbf{S}_{r,n}^H\left[\varepsilon_s\mathbf{H}_{sr,n}\mathbf{H}_{sr,n}^H+\mathbf{I}\sigma_{w1}^2\right]^{-1}\mathbf{S}_{r,n}, \end{aligned} \quad (18)$$

and $\mathrm{CRLB}(\mathbf{h}_{si})=\mathbf{J}^{-1}(\mathbf{h}_{si})$ is given by,

$$\mathrm{CRLB}(\mathbf{h}_{si})=\left(\mathbf{S}_{r,n}^H\left[\varepsilon_s\mathbf{H}_{sr,n}\mathbf{H}_{sr,n}^H+\mathbf{I}\sigma_{w1}^2\right]^{-1}\mathbf{S}_{r,n}\right)^{-1}.$$

The CRLB is independent of $\mathbf{H}_{si}$. However, it depends on $\mathbf{S}_{r,n}$ and $\mathbf{H}_{sr,n}$. Recalling that filtering matrix, $\mathbf{S}_{r,n}$ is given by equation (1) and noting that we are only concerned with the diagonal elements of the CRLB matrix, we end up with

$$[\mathrm{CRLB}(\mathbf{h}_{si})]_{ii}=\left\{\left(\mathbf{s}_{r,n}^{(i)}\right)^H\left[\varepsilon_s\mathbf{H}_{sr,n}\mathbf{H}_{sr,n}^H+\mathbf{I}\sigma_{w1}^2\right]^{-1}\mathbf{s}_{r,n}^{(i)}\right\}^{-1}.$$

Since $A>>M$, i.e., the number zero elements in $\mathbf{s}_{r,n}^{(M)}$ is too small to have any significant impact on the computations, from this point on, we will consider only $i=0$ in CRLB derivations: $\mathbf{s}_{r,n}^{(0)}=\mathbf{s}_{r,n}$. According to expressions (7) and (14), in the case of end-point equalization, $\mathbf{s}_{r,n}=\mathbf{H}_{sr,n-p}\mathbf{s}_{n-p}+\mathbf{w}_{1,n-p}+\mathbf{e}_{si,n-p}$, where $\mathbf{e}_{si,n-p}=\mathbf{x}_{si,n-p}-\hat{\mathbf{x}}_{si,n-p}=\mathbf{S}_{r,n-p}(\mathbf{h}_{si,n-p}-\hat{\mathbf{h}}_{si,n-p})=\mathbf{S}_{r,n-p}\mathbf{h}_{e,n-p}$ is the error vector for the estimation of $\mathbf{x}_{si,n-p}$.
In the noiseless case ($\sigma_{w1}^2=0$), we have

$$\mathrm{CRLB}(\mathbf{h}_{si})_{(\sigma_{w1}^2=0)}=\left(\mathbf{S}_{r,n-p}^H\left[\varepsilon_s\mathbf{H}_{sr,n}\mathbf{H}_{sr,n}^H\right]^{-1}\mathbf{S}_{r,n-p}\right)^{-1} \quad (19)$$

$$\begin{aligned}&\left[\mathrm{CRLB}(\mathbf{h}_{si})_{\text{end-point},(\sigma_{w1}^2=0)}\right]_{00}=\\ &\varepsilon_s\left\{\mathbf{s}_{n-p}^H\mathbf{H}_{sr,n-p}^H\left[\mathbf{H}_{sr,n}\mathbf{H}_{sr,n}^H\right]^{-1}\mathbf{H}_{sr,n-p}\mathbf{s}_{n-p}\right.\\ &\left.+\,\mathbf{s}_{r,n-p}^H\mathbf{H}_{e,n-p}^H\left[\mathbf{H}_{sr,n}\mathbf{H}_{sr,n}^H\right]^{-1}\mathbf{H}_{e,n-p}\mathbf{s}_{r,n-p}\right\}^{-1}, \end{aligned} \quad (20)$$

where, assuming sufficiently small estimation error, $\mathbf{H}_{e,n-p}$, the second term becomes negligible:

$$\begin{aligned}&\left[\mathrm{CRLB}(\mathbf{h}_{si})_{\text{end-point},(\sigma_{w1}^2=0)}\right]_{00}\approx\\ &\varepsilon_s\left\{\mathbf{s}_{n-p}^H\mathbf{H}_{sr,n-p}^H\left[\mathbf{H}_{sr,n}\mathbf{H}_{sr,n}^H\right]^{-1}\mathbf{H}_{sr,n-p}\mathbf{s}_{n-p}\right\}^{-1}. \end{aligned} \quad (21)$$

Applying the same logic in the case of distributed model,

$$\begin{aligned}&\left[\mathrm{CRLB}(\mathbf{h}_{si})_{distrib,(\sigma_{w1}^2=0)}\right]_{00}=\\ &\varepsilon_s\left\{\mathbf{s}_{n-p}^H\mathbf{H}_{sr,n-p}^H\mathbf{H}_{eq1,n-p}^H\left[\mathbf{H}_{sr,n}\mathbf{H}_{sr,n}^H\right]^{-1}\right.\\ &\times\,\mathbf{H}_{eq1,n-p}\mathbf{H}_{sr,n-p}\mathbf{s}_{n-p}+\mathbf{s}_{r,n-2p}^H\mathbf{H}_{e,n-p}^H\mathbf{H}_{eq1,n-p}^H\\ &\left.\times\,\left[\mathbf{H}_{sr,n}\mathbf{H}_{sr,n}^H\right]^{-1}\mathbf{H}_{eq1,n-p}\mathbf{H}_{e,n-p}\mathbf{s}_{r,n-2p}\right\}^{-1}. \end{aligned} \quad (22)$$

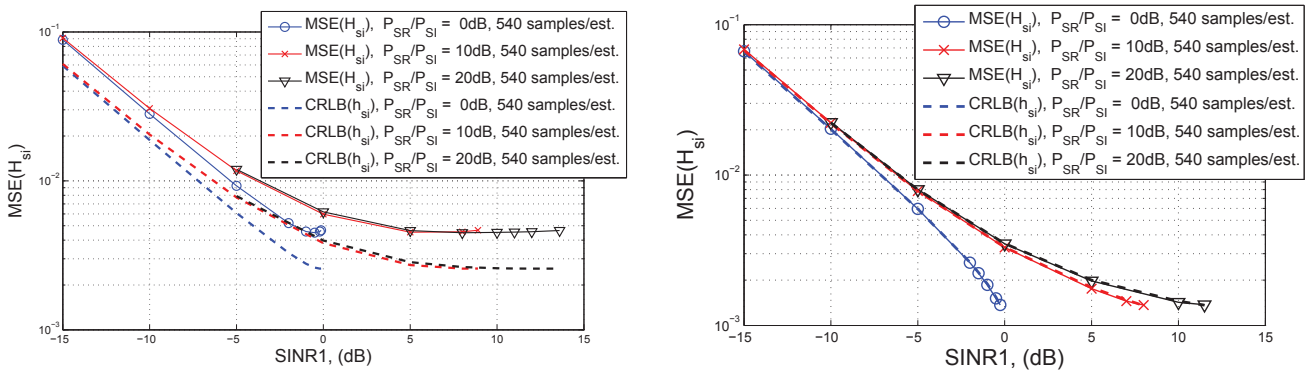

Fig. 2. $MSE(h_{si})$ for Full-duplex relay link with end-point (left) and distributed equalization (right)

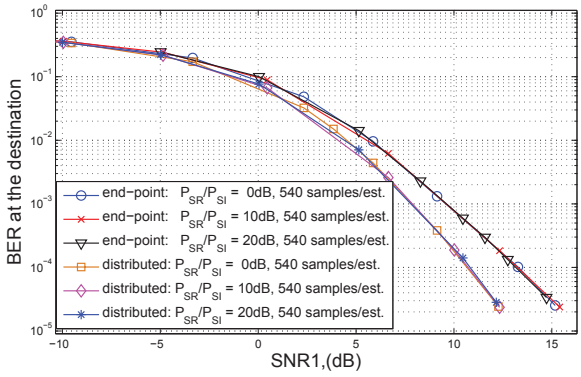

Fig. 3. BER performance for Full-duplex relay link with end-point and distributed equalization with SI cancellation enabled

$$\left[\text{CRLB}(\mathbf{h}_{si})_{distrib,(\sigma^2_{w1}=0)}\right]_{00} \approx \varepsilon_s\left\{\mathbf{s}^H_{n-p}\mathbf{H}^H_{sr,n-p}\mathbf{H}^H_{eq1,n-p}\left[\mathbf{H}_{sr,n}\mathbf{H}^H_{sr,n}\right]^{-1} \times \mathbf{H}_{eq1,n-p}\mathbf{H}_{sr,n-p}\mathbf{s}_{n-p}\right\}^{-1}. \quad (23)$$

Next, assuming both noiseless case and perfect equalization of SR channel, the above expression becomes:

$$\left[\text{CRLB}_{distrib,(\sigma^2_{w1}=0,\hat{H}_{sr}=H_{sr})}\right]_{00} \approx \varepsilon_s\left\{\mathbf{s}^H_{n-p}\left[\mathbf{H}_{sr,n}\mathbf{H}^H_{sr,n}\right]^{-1}\mathbf{s}_{n-p}\right\}^{-1}. \quad (24)$$

Under these conditions, the denominator of the CRLB is approximately given by,

End-point equalization:

$$\mathbf{s}^H_{n-p}\mathbf{H}^H_{sr,n-p}\left[\mathbf{H}_{sr,n}\mathbf{H}^H_{sr,n}\right]^{-1}\mathbf{H}_{sr,n-p}\mathbf{s}_{n-p} \quad (25)$$

Distributed equalization: $$\mathbf{s}^H_{n-p}\left[\mathbf{H}_{sr,n}\mathbf{H}^H_{sr,n}\right]^{-1}\mathbf{s}_{n-p} \quad (26)$$

Comparing equations (25) and (26) and noting that matrix $\left[\mathbf{H}_{sr,n}\mathbf{H}^H_{sr,n}\right]^{-1}$ has more negligible off-diagonal elements than matrix $\mathbf{H}^H_{sr,n-p}\left[\mathbf{H}_{sr,n}\mathbf{H}^H_{sr,n}\right]^{-1}\mathbf{H}_{sr,n-p}$, it is apparent that in high SNR conditions, the distributed equalization results in greater value of the denominator and hence lower value of $[CRLB]_{ii}$. These conclusions are in agreement with the simulation results discussed in the next section.

IV. Simulation Results

A. Simulation framework description

The blocks implemented within the simulation framework are shown in Fig. 1, where the equalizer block, $\mathbf{h}_{eq1}$, is present at the relay only in the case of distributed configuration. Data frames consisting of 540 symbols were used to compute each estimate of the SI channel, and the channel realization was assumed to be constant during this interval. Fractionally-spaced MMSE equalization with oversampling factor of 4 was used at the destination and, in the case of distributed model, at the relay. Constant SNR level of 20dB was configured at the destination receiver, while SINR sweeps at the relay receiver were performed. The SI channel estimation and BER performance is evaluated at the following three signal-to-self-interference levels: $\frac{P_{sr}}{P_{si}} = 0, 10, 20dB$.

B. SI channel estimation performance

The mean-square error and CRLB for SI channel estimation are plotted in Fig. 2. According to the figure, the LLSE-based SI channel estimator is able to achieve the CRLB in the case of the distributed model and almost achieve it in the case of end-point equalization. These results are expected under assumed conditions of complex Gaussian impairments. The plots also indicate that at high SNR, the CRLB is lower for the distributed model by a factor of approximately 2.

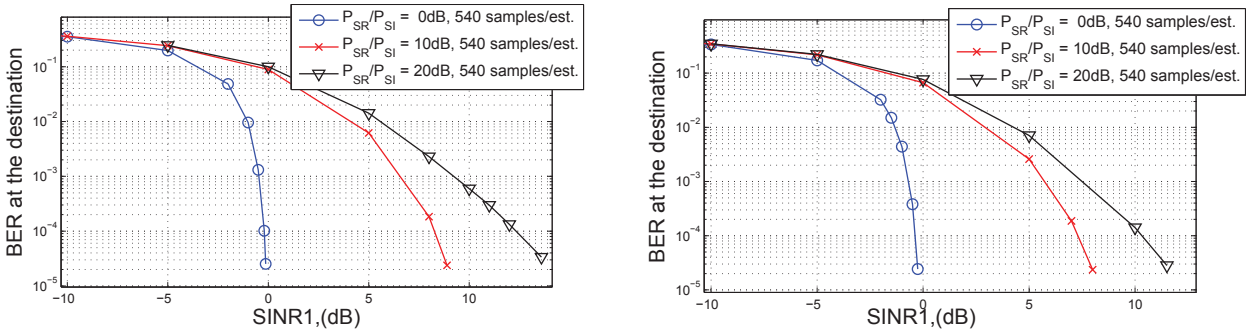

Fig. 4. BER performance for Full-duplex relay link with end-point (left) and distributed equalization (right) with SI cancellation enabled

C. End-to-end BER performance of end-point and distributed models:

Fig. 4 captures BER performance plotted against SINR at the relay receiver for three SI levels. Somewhat counter to intuition, in both cases, end-point and distributed, the BER performance improves with the increase in SI level. However, this can be easily explained by noting that for the fixed SINR level, according to equation (4), increase in the SI level, γ_{si}^2, results in equivalent reduction in the noise level. Since SI can be significantly reduced using SI cancellation, but noise cannot be reduced, the performance improves as we increase SI while reducing the AWGN energy.

Fig. 3 is based on the BER data from Fig. 4. However, in Fig. 3, the x-axis was changed to represent SNR at the relay receiver (instead of SINR). The SNR values were computed based on the SINR values of Fig. 4 using equation (5). The fact that the curves corresponding to the same equalization model but different $\frac{P_{sr}}{P_{si}}$ levels overlap in Fig. 3, confirms the earlier assertion that the SI cancellation results in the same cancellation error for each of the three $\frac{P_{sr}}{P_{si}}$ levels. Finally, according to simulation results in Fig. 3, for $\frac{P_{sr}}{P_{si}} = 0, 10, 20$dB, the distributed configuration is able to achieve lower BER than end-point model. Specifically, at BER$= 10^{-4}$, distributed model outperforms end-point model by 2.5dB.

V. Conclusion

In this paper, two channel equalization models were compared in the context of full-duplex relaying with residual self-interference. Three signal-to-residual self-interference levels were considered, and in all three cases, the distributed equalization model demonstrated better end-to-end BER performance than end-point equalization.

The CRLB for the SI channel estimation was also derived for each of the two models. The CRLB predicted better SI channel estimation performance at high SNR for distributed model and was in agreement with the simulation results.

Even though relatively simple MMSE-based SR and RD channel equalization scheme was assumed, simulation results indicate that the proposed distributed equalization model in conjunction with the LLSE-based residual SI cancellation could provide viable system performance assuming robust estimation performance of SR and RD channels.

References

[1] M. Duarte, C. Dick, and A. Sabharwal, "Experiment-driven characterization of full-duplex wireless systems," *IEEE Transactions on Wireless Communications*, 2012.

[2] S. Goyal, P. Liu, S. Hua, and S. Panwar, "Analyzing a full-duplex cellular system," in *2013 47th Annual Conference on Information Sciences and Systems (CISS)*, March 2013, pp. 1–6.

[3] M. Heino, D. Korpi, T. Huusari, E. Antonio-Rodriguez, S. Venkatasubramanian, T. Riihonen, L. Anttila, C. Icheln, K. Haneda, R. Wichman, and M. Valkama, "Recent advances in antenna design and interference cancellation algorithms for in-band full duplex relays," *IEEE Communications Magazine*, vol. 53, no. 5, pp. 91–101, May 2015.

[4] S. Kay, *Fundamentals of statistical signal processing: estimation theory*. Prentice Hall, 1993.

[5] D. Korpi, J. Tamminen, M. Turunen, T. Huusari, Y. S. Choi, L. Anttila, S. Talwar, and M. Valkama, "Full-duplex mobile device: pushing the limits," *IEEE Communications Magazine*, vol. 54, no. 9, pp. 80–87, September 2016.

[6] P. Lioliou, M. Viberg, M. Coldrey, and F. Athley, "Self-interference suppression in full-duplex mimo relays," in *2010 Conference Record of the Forty Fourth Asilomar Conference on Signals, Systems and Computers*, Nov 2010, pp. 658–662.

[7] T. Riihonen, S. Werner, and R. Wichman, "Comparison of full-duplex and half-duplex modes with a fixed amplify-and-forward relay," in *2009 IEEE Wireless Communications and Networking Conference*, April 2009, pp. 1–5.

[8] ——, "Mitigation of loopback self-interference in full-duplex mimo relays," *IEEE Transactions on Signal Processing*, vol. 59, no. 12, pp. 5983–5993, Dec 2011.

[9] T. Riihonen, S. Werner, R. Wichman, and E. Z. B., "On the feasibility of full-duplex relaying in the presence of loop interference," in *2009 IEEE 10th Workshop on Signal Processing Advances in Wireless Communications*, June 2009, pp. 275–279.

[10] T. Riihonen, S. Werner, and R. Wichman, "Residual self-interference in full-duplex mimo relays after null-space projection and cancellation," *2010 Conference Record of the Forty Fourth Asilomar Conference on Signals, Systems and Computers*, 2010.

[11] ——, "Mitigation of loopback self-interference in full-duplex mimo relays," *IEEE Transactions on Signal Processing*, 2011.

[12] S. Shao, D. Liu, K. Deng, Z. Pan, and Y. Tang, "Analysis of carrier utilization in full-duplex cellular networks by dividing the co-channel interference region," *IEEE Communications Letters*, vol. 18, no. 6, pp. 1043–1046, June 2014.

[13] Z. Ting, W. Fang, X. Jing, and J. Lilleberg, "Soft symbol estimation and forward scheme for cooperative relaying," in *2009 IEEE 20th International Symposium on Personal, Indoor and Mobile Radio Communications*, Sept 2009, pp. 3069–3073.

[14] Y. Tong, *The Multivariate Normal Distribution*. Springer New York, 1990.

[15] Z. Zhang, Y. Shen, S. Shao, W. Pan, and Y. Tang, "Full duplex 2×2 mimo radios," in *2014 Sixth International Conference on Wireless Communications and Signal Processing (WCSP)*, Oct 2014, pp. 1–6.